Inorganic Chemistry
Communication
pubs.acs.org/IC

$Ag(nic)_2$ (nic = Nicotinate): A Spin-Canted Quasi-2D Antiferromagnet Composed of Square-Planar $S = {}^1/_2$ Ag^{II} Ions

Jamie L. Manson,*[†] Toby J. Woods,[†] Saul H. Lapidus,[‡] Peter W. Stephens,[‡] Heather I. Southerland,[†] Vivien S. Zapf,[§] John Singleton,[§] Paul A. Goddard,[⊥] Tom Lancaster,[⊥] Andrew J. Steele,[⊥] and Stephen J. Blundell[⊥]

[†]Department of Chemistry and Biochemistry, Eastern Washington University, Cheney, Washington 99004, United States
[‡]Department of Physics and Astronomy, State University of New York, Stony Brook, New York 11794, United States
[§]National High Magnetic Field Laboratory, Los Alamos National Laboratory, Los Alamos, New Mexico 87545, United States
[⊥]Clarendon Laboratory, Department of Physics, University of Oxford, Oxford OX1 3PU, U.K.

Supporting Information

ABSTRACT: Square-planar $S = {}^1/_2$ Ag^{II} ions in polymeric $Ag(nic)_2$ are linked by bridging nic monoanions to yield 2D corrugated sheets. Long-range magnetic order occurs below $T_N = 11.8(2)$ K due to interlayer couplings that are estimated to be about 30 times weaker than the intralayer exchange interaction.

Pyridinecarboxylate ligands, and especially nicotinate (nic), have been used extensively in the self-assembly of 1-, 2-, and 3D polymeric architectures. This is because nic can serve as an effective bridging function (through pyridine N and carboxylate O atoms) between transition-metal cations.[1−3] Structurally characterized examples include, but are not limited to, $M(nic)_2$ (M = Mn,[1a] Fe,[1b] Co,[1c] and Cu[1d]), $Ni_2(nic)_4(H_2O)$,[2a] $Co(nic)_2(H_2O)$,[2b] $Mn(nic)_2(H_2O)_2$,[2c] $Ni(nic)_2(H_2O)_4$[2d] and Ag(nic)(nicH)[3] among others. For $M(nic)_2$, M = Mn, Fe, and Co are characterized by six-coordinate MO_4N_2 centers connected to other sites via either μ- or μ_3-coordination or a combination thereof. $Cu(nic)_2$ has distorted five-coordinate CuO_3N_2 units, with each nic anion being ligated through the N atom and both O atoms to three different Cu ions.[1d] The few reports on their magnetic properties indicated only weak exchange interactions and the absence of long-range magnetic ordering (LRO) above 2 K.

Although the $S = {}^1/_2$ Ag^{II} ion is generally oxygen-sensitive, Banerjee and Ray reported the synthesis of $Ag(nic)_2$ in 1956 and noted that it could remain stable for several months so long as the powder was kept dry.[4] Early powder X-ray diffraction studies on $Ag(nic)_2$ suggested a tetragonal symmetry, although a detailed structural analysis was not carried out.[5] Adopting a slightly modified preparation method (see SI), samples were prepared at low temperature and stored in a refrigerator; unlike $Ag(pyz)_2(S_2O_8)$,[6] we ultimately found $Ag(nic)_2$ to be air-stable at room temperature.

Herein, we report on the crystal structure and magnetism of $Ag(nic)_2$. Using X-rays at the National Synchrotron Light Source (Brookhaven National Laboratory), the crystal structure of $Ag(nic)_2$ was solved from powder X-ray diffraction data[7,8] (see Figure S1). The Ag^{II} ion has square-planar D_{2h} symmetry and occupies an inversion center. The coordination sphere consists of two O atoms [Ag1−O1 = 2.18(1) Å] and two N atoms [Ag1−N1 = 2.195(5) Å] that belong to four different nic anions. A second carboxylate O atom lies 2.95 Å away and is only weakly interacting [$\sum$vdw = 1.72 (Ag) + 1.52 (O) = 3.24 Å]. The AgO_2N_2 plane exhibits a nearly ideal O1−Ag1−N1 bond angle of 89.7(2)°, and the Ag1−O1−C6 bond angle formed upon coordination of the carboxylate O1 atom is 108.9(6)°. The carboxylate moiety makes a torsion angle of 12.4° relative to the pyridine ring.

$Ag(nic)_2$ consists of extended 2D polymeric networks (Figure 1). Every AgO_2N_2 unit is connected to four others

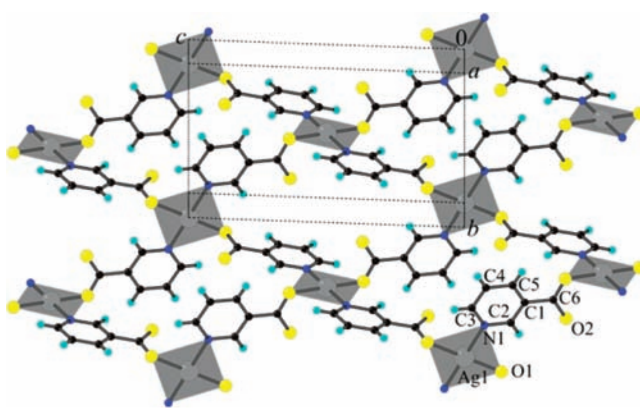

Figure 1. Portion of a 2D polymeric sheet as found in $Ag(nic)_2$.

via bridging nic anions to form a rhombically distorted square array of equidistant Ag^{II} ions (Ag···Ag = 8.205 Å). The proximity of the N atom and carboxylate moiety on the nic anion leads to corrugated sheets such that every other AgO_2N_2 unit adopts the same orientation. The sheets in $Cu(nic)_2$ are also pleated but not in the same way as $Ag(nic)_2$ because of the differences in nic and Cu^{II} ion coordination.

Adjacent 2D sheets pack *in*-registry along the [$\bar{1}$01] direction (Figure S2) whereby AgO_2N_2 planes stack directly above and below other AgO_2N_2 units of the same spatial orientation. The

Received: December 2, 2011
Published: January 27, 2012

closest interlayer Ag···Ag spacing is 5.016 Å. The structure of $Ag(nic)_2$ represents a new topology among $M(nic)_2$ coordination polymers.

The magnetic susceptibility, $\chi(T)$, for $Ag(nic)_2$ was measured in a 0.1 T direct-current (dc) magnetic field (Figure 2a). χ gradually increases as the temperature is lowered, passing through a broad maximum at T_{max} = 28.7 K. For low-dimensional magnetic systems, the presence of a broad maximum typically signifies short-range spin correlations due to the largest exchange interaction, in this case, between $S = {}^1/_2$ Ag^{II} ions within layers. Below T_{max}, χ continues to decrease until a second weak peak occurs at 11.5 K, which we ascribe to 3D long-range magnetic order (T_N), with the energy scale set by a weaker interlayer interaction. It is interesting to note that such a feature is completely absent in $Ag(pyz)_2(S_2O_8)$[6] and may originate from a larger interlayer coupling and/or canting of the magnetic moments in $Ag(nic)_2$. The notion of spin canting in $Ag(nic)_2$ is supported by the field dependence of $M(T)$ in the vicinity of the 11.5 K feature (Figure 2b), whereas the 28 K feature remains broad and does not shift with the field.

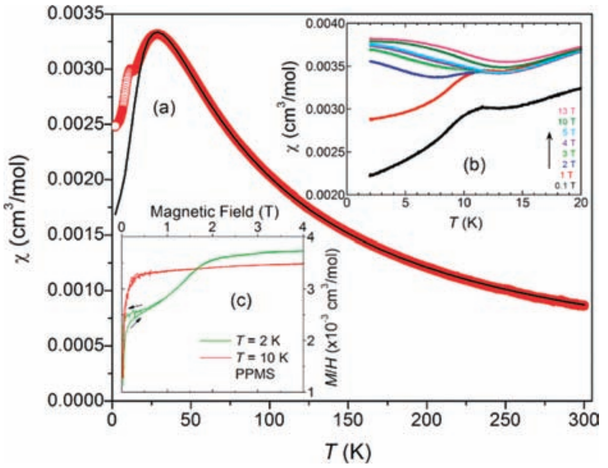

Figure 2. (a) Magnetic susceptibility data for $Ag(nic)_2$ measured at H_{dc} = 0.1 T. The solid line is a theoretical fit to the data as described in the text. (b) $M(T)$ between 2 and 20 K for several H. (c) $M(H)$ obtained at 1.5 and 4.1 K for pulsed fields up to 60 T.

An estimate of the relative strength of magnetic interactions in $Ag(nic)_2$ can be gleaned from a fit ($100 \leq T \leq 300$ K) of the reciprocal magnetic susceptibility, $1/\chi(T)$ (not shown), to a Curie–Weiss law, where $1/\chi = 8(T - \theta)/N\mu_B{}^2g^2S(S + 1)$. The fitted parameters were g = 2.12(1) and θ = −46.0(1) K, where $\theta < 0$ is consistent with antiferromagnetic (AFM) coupling between $S = {}^1/_2$ Ag^{II} sites. $\chi(T)T$ (not shown) strongly decreases over the whole T range, which is consistent with strong AFM interactions.

The intrinsic two-dimensionality of the crystal structure, as well as the plausible Heisenberg behavior of the Ag^{II} ion and the negative Weiss constant, calls for an AFM Heisenberg model based on a square lattice. Accordingly, the $\chi(T)$ data presented in Figure 2a were fitted[9] over the 16–300 K temperature range (i.e., above T_N) to yield satisfactory agreement for g = 2.10(1) and J/k_B = 30.3(1) K based on the spin Hamiltonian $\hat{H} = J\sum S_i \cdot S_j$ where $J > 0$ indicates AFM coupling. The resulting J value is in line with the temperature of the peak susceptibility, $T_{max} = 0.936J$ = 28.4 K, obtained from high-temperature series expansions.[10] $Ag(nic)_2$ displays much stronger AFM coupling than $Cu(nic)_2$ (J = 12.8 K), despite the presence of shorter Cu−O−C−O−Cu exchange paths in the latter.[1d] Together, the nonlinear Ag−nic−Ag pathways and longer Ag···Ag separations in $Ag(nic)_2$ afford smaller AFM coupling relative to $Ag(pyz)_2(S_2O_8)$ where J = 53 K.[6]

The bulk magnetic behavior of $Ag(nic)_2$ can be rationalized by considering the likely exchange pathways. In this system, the magnetic d_{x2-y2} orbital of Ag^{II} overlaps with the lone pairs of electrons belonging to N1 and O1 of the bridging nic anion. The exchange interaction is mediated between adjacent Ag^{II} ions via the σ-bonding network provided by the bridging ligands. The d_{z2} orbital is spin-paired, lies orthogonal to the AgO_2N_2 plane, and cannot provide a suitable exchange pathway. Appreciable tilting of the AgO_2N_2 planes with respect to nearest-neighbors likely induces a staggered **g**-tensor, which affords a spin-canted ground state, as suggested by $M(H,T)$ data.

A strong magnetic coupling between Ag^{II} ions is evidenced by the pulsed-field magnetization data (Figure S3), whereby (i) a small moment was found and (ii) a very slightly concave $M(H)$ curve, typical of a quasi-2D $S = {}^1/_2$ Heisenberg antiferromagnet, was observed.[11] The latter characteristic persists to the highest available field, suggesting a saturation field (B_c) well above 60 T. From previous work, we found that the simple expression $gB_c/J \approx 6.03$ T/K[11] may be used to estimate B_c of a quasi-2D $S = {}^1/_2$ antiferromagnet based on the extracted g and J values obtained from the fit of $\chi(T)$. The extracted J value, known to describe Cu^{II} salts rather well, predicts $B_c \approx 87$ T for $Ag(nic)_2$. The $M(H)$ data suggest a higher critical field, perhaps due to an additional energy scale, or a significantly enhanced concavity of $M(H)$ above 60 T, which implies a lower magnetic dimensionality. Figure 2c clearly shows that by ∼1 and 2 T, respectively, the hysteresis between up/downfield sweeps and a spontaneous magnetic moment becomes quenched, whereas M/H grows nearly linear for larger H as a result of dominant in-plane AFM correlations.

Zero-field (ZF) muon-spin-rotation experiments were performed to confirm the suspected long-range magnetic order in $Ag(nic)_2$. Example spectra are shown in the inset of Figure 3. For $T > 12$ K, we observe monotonic relaxation, typical of $T > T_N$ behavior in materials of this type.[6,12] Below the AFM transition at T_N, we see oscillations in the time

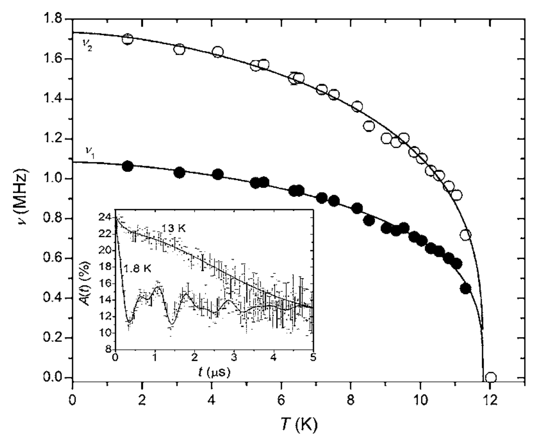

Figure 3. (Inset) ZF μ^+SR data measured at 1.8 and 13 K for $Ag(nic)_2$. Oscillations were observed for $T < 12$ K. (Main) T evolution of the muon precession frequencies in $Ag(nic)_2$. For both plots, the solid lines denote theoretical fits, as described in the text and SI.

dependence of the muon polarization [the "asymmetry" $A(t)$[13]], which are characteristic of a quasi-static local magnetic field at the muon stopping site. This provides very strong evidence for the existence of long-range magnetic order.[14]

The muon precession frequencies (ν), of which two exist in $Ag(nic)_2$, are proportional to the magnetic order parameter. Two muon precession frequencies are typically observed in molecular materials of this type. However, without a magnetic structure, it is difficult to reliably determine the muon stopping sites. In a recent paper,[14] we demonstrated that there are several plausible muon sites in one class of coordination polymers, some of which do not lead to measurable oscillations. Given that the role of the μSR measurements in this study was to determine the presence of LRO rather than an exhaustive analysis of the muon response, we will not speculate on their positions in this structure.

The T dependence of ν is shown in the main plot of Figure 3. The behavior may be parametrized by a fit to the phenomenological expression $\nu_i(T) = \nu_i(0)\ [1 - (T/T_N)^{\alpha}]^{\beta}$, from which we extract $\nu_1(0) = 1.08(1)$ MHz, $\nu_2(0) = 1.73(2)$ MHz, $T_N = 11.8(2)$ K, $\alpha = 1.5(3)$, and $\beta = 0.30(4)$. An increase in the nonoscillatory component near T_N makes it difficult to come to firm conclusions about the critical behavior of $Ag(nic)_2$.

ZF μ^+SR measurements were made up to 50 K, and there is no evidence for changes in the magnetic behavior around 28 K, the temperature at which $\chi(T)$ exhibits a maximum. In fact, we would not expect any; above T_N in these materials, the electronic moments typically fluctuate at a very rapid rate compared to the muon response time (determined by the muon gyromagnetic ratio) and are therefore motionally narrowed from the spectra. The muon relaxation above T_N is then caused by disordered nuclear moments. We therefore do not generally observe any feature in the muon spectra around T_{max} of $\chi(T)$, which is temperature-independent above T_N.

By combining the known T_N and J values, we estimated the interlayer magnetic interaction ($J_\perp$) using the 2D model obtained by Yasuda et al.[15] From the equation $\ln(J_\perp/J) = b - 4\pi\rho_s/T_N$, where $b = 2.43$ and $\rho_s = 0.183J$ for $S = {}^1/_2$, we calculate $|J_\perp/J| = 0.033$ or $|J_\perp| = 0.99$ K. The small $J_\perp$ is sufficient to facilitate the observed LRO that occurs.

In conclusion, $Ag(nic)_2$ has a unique 2D corrugated structure composed of alternately tilted square-planar AgO_2N_2 units that consist of Ag^{II} ($S = {}^1/_2$) centers. Magnetic data suggest that it is a quasi-2D Heisenberg antiferromagnet likely to exhibit a spin-canted ground state below $T_N = 11.8(2)$ K. A large AFM interaction occurs within the 2D layers, although the coupling is much weaker between them. To the best of our knowledge, $Ag(nic)_2$ is the first reported molecule-based Ag^{II}-containing spin-canted AFM.

■ ASSOCIATED CONTENT

Ⓢ Supporting Information

Synthesis, characterization details, layer packing diagram, high-field $M(H)$ plot, and CIF for $Ag(nic)_2$. This material is available free of charge via the Internet at http://pubs.acs.org.

■ AUTHOR INFORMATION

Corresponding Author

*E-mail: jmanson@ewu.edu.

Notes

The authors declare no competing financial interest.

■ ACKNOWLEDGMENTS

Work at EWU was supported by the U.S. National Science Foundation (NSF) under Grant DMR-1005825. Research carried out, in part, at the National Synchrotron Light Source at Brookhaven National Laboratory was supported by the U.S. Department of Energy (DoE), Office of Science, Basic Energy Sciences (BES), under Contract DE-AC02-98CH10886. A portion of this work was performed at the National High Magnetic Field Laboratory, which is supported by the NSF Cooperative Agreement DMR-0654118, the State of Florida, and the U.S. DoE BES program "Science in 100 T". Some of this work was carried out at the Swiss Muon Source, Paul Scherrer Institut, CH. This project was supported by the EPSRC (UK) and by the European Commission under the seventh Framework Program through the "Research Infrastructures" action of the "Capacities" Program, Contract CP-CSA INFRA-2008-1.1.1, No. 226507-NMI3. We are grateful to Alex Amato for experimental assistance.

■ REFERENCES

(1) (a) Lin, W.; Chapman, M. E.; Wang, Z.; Lee, G. T. *Inorg. Chem.* **2000**, *39*, 4169. (b) Ng, S. W. *Acta Crystallogr.* **2008**, *E64*, m728. (c) Feng, W.-J.; Zhou, G.-P.; Zheng, X.-F.; Liu, Y.-G.; Xu, Y. *Acta Crystallogr.* **2006**, *E62*, m2033. (d) Chapman, M. E.; Ayyappan, P.; Foxman, B. M.; Lee, G. T.; Lin, W. *Cryst. Growth Des.* **2001**, *1*, 159.

(2) (a) Wu, C.-D.; Lu, C.-Z.; Zhuang, H.-H.; Huang, J.-S. *Z. Anorg. Allg. Chem.* **2003**, *629*, 693. (b) Yeh, C.-W.; Suen, M.-C.; Hu, H.-L.; Chen, J.-D.; Wang, J.-C. *Polyhedron* **2004**, *23*, 1947. (c) Hao, X.; Wei, Y.-G.; Liu, Q.; Zhang, S.-W. *Acta Crystallogr.* **2000**, *C56*, 296. (d) Batten, S. R.; Harris, A. R. *Acta Crystallogr.* **2001**, *E57*, m9.

(3) Kall, P. O.; Grins, J.; Fahlman, M.; Soderlind, F. *Polyhedron* **2001**, *20*, 2747.

(4) Banerjee, B.; Ray, P. *J. Ind. Chem. Soc.* **1956**, *33*, 503.

(5) Chackraburtty, D. M. *Acta Crystallogr.* **1957**, *10*, 128.

(6) Manson, J. L.; Stone, K. H.; Southerland, H. I.; Lancaster, T.; Steele, A. J.; Blundell, S. J.; Pratt, F. L.; Baker, P. J.; McDonald, R. D.; Sengupta, P.; Singleton, J.; Goddard, P. A.; Lee, C.; Whangbo, M.-H.; Warter, M. L.; Mielke, C. H.; Stephens, P. W. *J. Am. Chem. Soc.* **2009**, *131*, 4590.

(7) (a) Bruker AXS. *TOPAS V4: General profile and structure analysis software for powder diffraction data User's Manual*; Bruker AXS: Karlsruhe, Germany, 2005. (b) Coelho, A. A. *J. Appl. Crystallogr.* **2003**, *36*, 86. (c) *TOPAS-Academic* is available at www.topas-academic.net.

(8) Structural data for $Ag(nic)_2$: empirical formula $C_{12}H_8AgN_2O_4$, M_r = 352.07, space group $P2_1/n$, T = 300 K, a = 5.0157(1) Å, b = 8.0371(2) Å, c = 14.1498(4) Å, β = 98.373(3)°, V = 564.33(2) Å^3, Z = 2, ρ = 2.072 g cm^{-3}; μ = 1.697 mm^{-1}; R_{wp} = 0.055 68, R_{exp} = 0.046 15. Further details of the structure solution and refinement are provided in the Supporting Information and CIF.

(9) Woodward, F. M.; Albrecht, A. S.; Wynn, C. M.; Landee, C. P.; Turnbull, M. M. *Phys. Rev. B* **2002**, *65*, 144412.

(10) Lines, M. E. *J. Phys. Chem. Solids* **1970**, *31*, 101.

(11) Goddard, P. A.; Singleton, J.; Sengupta, P.; McDonald, R. D.; Lancaster, T.; Blundell, S. J.; Pratt, F. L.; Cox, S.; Harrison, N.; Manson, J. L.; Southerland, H. I.; Schlueter, J. A. *New J. Phys.* **2008**, *10*, 083025.

(12) e.g. Manson, J. L.; Schlueter, J. A.; Funk, K. A.; Southerland, H. I.; Twamley, B.; Lancaster, T.; Blundell, S. J.; Baker, P. J.; Pratt, F. L.; Singleton, J.; McDonald, R. D.; Goddard, P. A.; Sengupta, P.; Batista, C. D.; Ding, L.; Lee., C.; Whangbo, M.-H.; Franke, I.; Cox, S.; Baines, C.; Trial, D. *J. Am. Chem. Soc.* **2009**, *131*, 6733.

(13) Blundell, S. J. *Contemp. Phys.* **1999**, *40*, 175.

(14) Steele, A. J.; Lancaster, T.; Blundell, S. J.; Baker, P. J.; Pratt, F. L.; Baines, C.; Conner, M. M.; Southerland, H. I.; Manson, J. L.; Schlueter, J. A. *Phys. Rev. B* **2011**, *84*, 064412.

(15) Yasuda, C.; Todo, S.; Hukushima, K.; Alet, F.; Keller, M.; Troyer, M.; Takayama, H. *Phys. Rev. Lett.* **2005**, *94*, 217201.